Eur. Phys. J. A **10**, 487–491 (2001)

THE EUROPEAN PHYSICAL JOURNAL A

Stopping power of low-energy deuterons in ^{3}He gas

F. Raiola[1], G. Gyürky[2], M. Aliotta[1,a], A. Formicola[1], R. Bonetti[3], C. Broggini[4], L. Campajola[5], P. Corvisiero[6], H. Costantini[6], A. D'Onofrio[7], Z. Fülöp[2], G. Gervino[8], L. Gialanella[5], A. Guglielmetti[3], C. Gustavino[9], G. Imbriani[5,10], M. Junker[9], R.W. Kavanagh[12], P.G.P. Moroni[6], A. Ordine[5], P. Prati[6], V. Roca[5], D. Rogalla[1], C. Rolfs[1,b], M. Romano[5], F. Schümann[1], E. Somorjai[2], O. Straniero[11], F. Strieder[1], F. Terrasi[7], H.P. Trautvetter[1], and S. Zavatarelli[6]

[1] Institut für Physik mit Ionenstrahlen, Ruhr-Universität Bochum, Bochum, Germany
[2] Atomki, Debrecen, Hungary
[3] Dipartimento di Fisica, Università di Milano and INFN, Milano, Italy
[4] INFN, Padova, Italy
[5] Dipartimento di Scienze Fisiche, Università Federico II and INFN, Napoli, Italy
[6] Dipartimento di Fisica, Università di Genova and INFN, Genova, Italy
[7] Dipartimento di Scienze Ambientali, Seconda Università di Napoli, Caserta and Napoli, Italy
[8] Dipartimento di Fisica Sperimentale, Università di Torino and INFN, Torino, Italy
[9] Laboratori Nazionali del Gran Sasso dell'INFN, Assergi, Italy
[10] Osservatorio Astronomico di Capodimonte, Napoli, Italy
[11] Osservatorio Astronomico di Collurania, Teramo, Italy
[12] California Institute of Technology, Pasadena, CA, USA

Received: 14 February 2001 / Revised version: 20 April 2001
Communicated by D. Schwalm

Abstract. The stopping power of atomic and molecular deuterons in ^{3}He gas was measured over the range $E_\mathrm{d} = 10$ to 100 keV using the ^{3}He pressure dependence of the ^{3}He(d,p)^{4}He reaction yield. At energies above 30 keV, the observed stopping power values are in good agreement with a standard compilation. However, near 18 keV the experimental values drop by a factor 50 below the extrapolated values of the compilation. In a simple model, the behavior is due to the minimum $1s \rightarrow 2s$ electron excitation of the He target atoms (= 19.8 eV, corresponding to $E_\mathrm{d} = 18.2$ keV), *i.e.* it is a quantum effect, by which the atoms become nearly transparent for the ions.

PACS. 26.20.+f Hydrostatic stellar nucleosynthesis – 34.50.-s Scattering of atoms and nucleus

1 Introduction

Due to the Coulomb barrier of the entrance channel, the cross-section $\sigma(E)$ of a fusion reaction drops exponentially with decreasing center-of-mass energy E,

$$\sigma(E) = S(E)E^{-1}\exp[-2\pi\eta]\,, \tag{1}$$

where η is the Sommerfeld parameter and $S(E)$ is the astrophysical S-factor [1,2]. For $\sigma(E)$ measurements at subcoulomb energies, an accurate knowledge of the effective beam energy associated with the observed reaction yield is as important as the yield measurements themselves. In the analysis of such data, the effective energy in the target always involves energy-loss corrections, which are usually extracted from a standard compilation [3]. The compilation is based on experimental data down to energies around the Bragg peak, while at lower energies —relevant to nuclear astrophysics— no data exist; thus, the data obtained at higher energies are extrapolated to lower energies with theoretical guidance. In recent studies of the d(^{3}He,p)^{4}He reaction ($Q = 18.4$ MeV) at the LUNA facility [4], the observed stopping power of ^{3}He ions in D_2 molecular gas was in good agreement with the extrapolated values of the compilation. For studies of the inverted reaction, *i.e.* ^{3}He(d,p)^{4}He, stopping power data are needed for deuterons in He gas: measurements —using time-of-flight spectrometry— indicated [5] significantly lower values than tabulated [3]. We restudied the ^{3}He(d,p)^{4}He low-energy cross-section including a measurement of the associated stopping power. We report here on the latter part only; preliminary results have been published [6].

[a] Alexander von Humboldt Fellow
[b] e-mail: rolfs@ep3.ruhr-uni-bochum.de

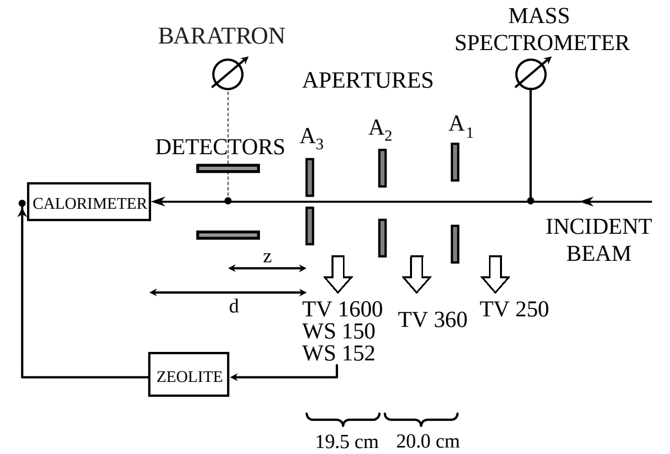

Fig. 1. Schematic diagram of the experimental setup. The ion beam enters the target chamber through the apertures A_1, A_2 and A_3 of high pumping impedance and is stopped in a calorimeter. The differentially pumping stages consist of turbo pumps (*e.g.*, TV1600 = 1600 l/s pumping speed) and Roots blowers (*e.g.*, WS150 = 150 m^3/h pumping speed). The ^{3}He gas from the 3 pumping stages is passed through a zeolite trap cooled to liquid nitrogen temperature and fed back into the target chamber. The gas pressure at the location of the detectors is measured with a Baratron capacitance manometer. The gas composition is monitored using a mass spectrometer.

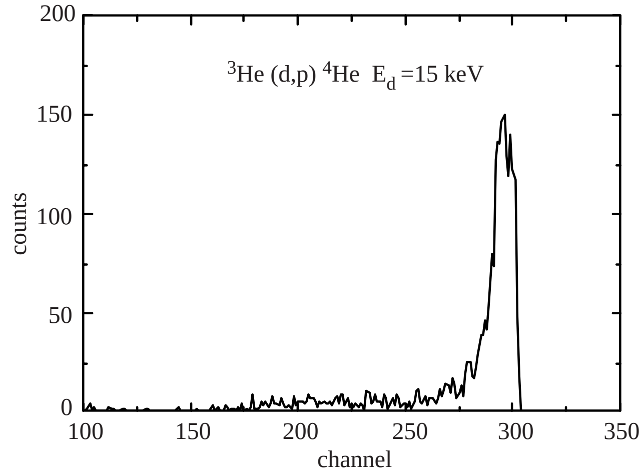

Fig. 2. Spectrum for the ^{3}He(d,p)^{4}He reaction (Q = 18.4 MeV) obtained at $E_{\rm d}$ = 15 keV. The peak corresponds to the 14.7 MeV protons fully stopped in the Si detector, while the low-energy tail represents protons losing only a fraction of their energy in the detector. The reaction yield was deduced from the number of counts in both the peak and the tail.

2 Setup and procedures

Details of the experimental setup (fig. 1) and procedures have been reported [6] and we describe here only differences and details not reported previously. The energy spread of the incident deuteron beam was found to be 0.10 keV at $E_{\rm d}$ = 20 keV. The detector setup consisted of four, 1 mm thick Si detectors of 5×5 cm^2 area (each) placed around the beam axis: they formed a 5 cm long parallelepiped in the target chamber, by which solid angle effects due to beam misalignment or angle straggling of the beam are minimised. A NE102A plastic scintillator (1×1 m^2 area, 3.5 cm thickness; not shown in fig. 1) was placed below the target chamber and used to veto cosmic-ray–induced events in the detectors. A sample spectrum is illustrated in fig. 2.

At a given incident deuteron energy $E_{\rm d}$, the reaction yield $Y(E_{\rm d}, P) \propto NW^{-1}P^{-1}$ was obtained as a function of gas pressure P, where N is the number of observed protons from the reaction ^{3}He(d,p)^{4}He (in the detector setup) and W is the integrated beam power (deduced from the calorimeter). The pressure-dependent yield is given by the expression [6]

$$\alpha Y(E_{\rm d}, P) = (1 + \varepsilon(E_{\rm d})\rho_{\rm o} P d P_{\rm o}^{-1} E_{\rm d}^{-1}) \times (1 - \varepsilon(E_{\rm d})\rho_{\rm o} z(\pi \quad \eta - 1) P P_{\rm o}^{-1} E_{\rm d}^{-1} + \dots), \qquad (2)$$

where α is a normalisation constant containing all pressure-independent quantities, z and d are distances defined in fig. 1, $\varepsilon(E_{\rm d})$ is the stopping power of deuterons in the ^{3}He gas, $\rho_{\rm o}$ and $P_{\rm o}$ are the density and pressure of the ^{3}He gas at STP, respectively. Since relative yield measurements are performed, the normalisation constant α was chosen such that $Y(E_{\rm d}, P \to 0) = 1$. In eq. (2) the terms $S(E)$ and $\varepsilon(E)$ are constant over the energy range Δ of the target thickness. A constant $S(E)$ value over Δ is justified [7] including the effects of electron screening in eqs. (1) and (2) (less than 1% change in $S(E)$ over $\Delta(1\ {\rm mbar}) = 0.4$ keV at $E_{\rm d}$ = 18 keV). However, the values of the stopping power $\varepsilon(E)$ are somewhat energy dependent over Δ (sect. 3). Simulations, including the effects of folding the cross-section with the detection efficiency along the beam axis, have shown that this energy dependence leads to an error comparable to the experimental uncertainty and thus has been neglected. The simulations, which included also the effects of energy and angle straggling, have shown that the stopping power value deduced from eq. (2) is an acceptable number within experimental uncertainty. Since relative values of the cross-section are involved here, only statistical and accidental errors have to be included in the analysis.

3 Results

In one set of experiments, an atomic deuteron beam (D_1^+) at $E_{\rm d}$ = 13 to 100 keV was used (8 μA maximum current on target at $E_{\rm d}$ = 13 keV). The example shown in fig. 3 for the pressure-dependent yield of ^{3}He(d,p)^{4}He at $E_{\rm d}$ = 25 keV led to $\varepsilon = (2.93 \pm 0.10) \times 10^{-15}$ eVcm^2 or $\varepsilon/\varepsilon_{\rm comp} = 0.89 \pm 0.03$ (table 1), where $\varepsilon_{\rm comp}$ is the value from the compilation [3]. The deduced stopping power values are summarized in table 1 and displayed in fig. 4a, where the results in form of the ratio $\varepsilon/\varepsilon_{\rm comp}$ are compared with the values from the compilation.

In another set of experiments, diatomic deuteron beams (D_2^+) at energies 24 to 100 keV were used (30 μA

Table 1. Stopping power ε of deuterons in ^{3}He gas.

$E_{\rm d}^{\rm a}$ (keV)	$\varepsilon_{\rm comp}^{\rm b}$ (10^{-15} eVcm^2)	$\varepsilon/\varepsilon_{\rm comp}^{\rm c}$
	atomic deuterons (D_1^+)	
100	6.984	1.01±0.03
90	6.735	1.02±0.03
80	6.409	1.00±0.03
70	6.001	1.01±0.03
60	5.510	1.03±0.03
50	4.939	0.99±0.03
40	4.306	0.98±0.04
30	3.631	1.03±0.03
25	3.290	0.89±0.03
22.5	3.122	0.78±0.03
20	2.958	0.64±0.04
19	2.909	0.53±0.03
18	2.861	0.44±0.04
17	2.810	0.40±0.05
16	2.757	0.39±0.05
15	2.702	0.19±0.04
13	2.586	0.13±0.07
	diatomic deuterons (D_2^+)	
50	4.939	1.01±0.03
40	4.306	0.95±0.04
30	3.631	1.02±0.03
25	3.290	0.83±0.04
22.5	3.122	0.75±0.03
20	2.958	0.56±0.04
19	2.909	0.53±0.03
18	2.861	0.49±0.04
17	2.810	0.43±0.04
16	2.757	0.38±0.04
15	2.702	0.25±0.08
14	2.645	0.19±0.08
12	2.524	0.07±0.06
	triatomic deuterons (D_3^+)	
30	3.631	0.92±0.04
25	3.290	0.78±0.04
22.5	3.122	0.77±0.03
20	2.958	0.61±0.03
19	2.909	0.57±0.03
18	2.861	0.43±0.03
17	2.810	0.42±0.05
16	2.757	0.38±0.04
15	2.702	0.26±0.03
14	2.645	0.20±0.04
13	2.586	0.09±0.04
12	2.524	0.06±0.03
11	2.460	0.02±0.03
10	2.393	0.019±0.019

[a] Equivalent atomic deuteron energy in case of molecular deuterons.
[b] From the compilation SRIM-2000.39 [3].
[c] Errors include statistical and accidental uncertainties in gas pressure (*e.g.*, beam heating effects) and beam power.

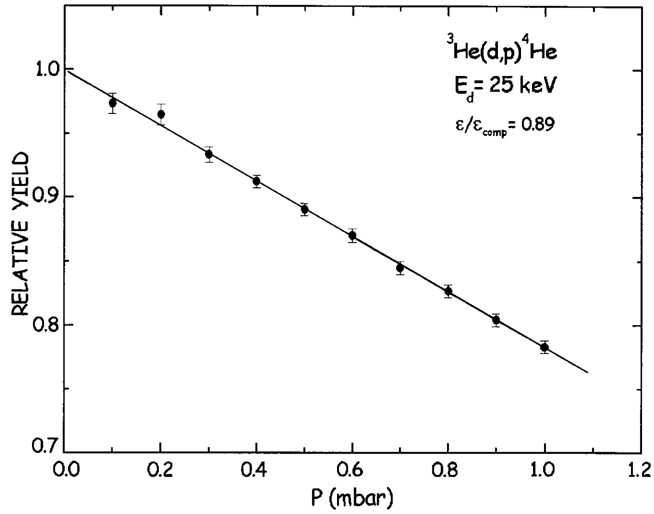

Fig. 3. Relative yield of ^{3}He(d,p)^{4}He as a function of ^{3}He gas pressure P at $E_{\rm d}$ = 25 keV. The solid line through the data points is a fit assuming a linear pressure dependence, where the resulting stopping power ratio $\varepsilon/\varepsilon_{\rm comp}$ ($\varepsilon_{\rm comp}$ from the compilation [3]) is given.

maximum current at 24 keV). Since the molecular beam breaks up quickly in the upstream part of the ^{3}He target gas (1.5 cm mean free path for P = 0.5 mbar, *i.e.* break-up within the entrance aperture A_3), an equivalent deuteron beam of $E_{\rm d}$ = 12 to 50 keV is produced with a nearly twofold increase in current. The energy spread $\Delta E_{\rm d}$ of the resulting deuteron beam due to the effects of Coulomb explosion of the molecular beam is estimated to be at most $\Delta E_{\rm d}$ = 0.69 keV at $E_{\rm d}$ = 20 keV. Since the Coulomb explosion has been found to be "gentle" [8–12], the actual spread $\Delta E_{\rm d}$ is significantly smaller. The resulting ratios $\varepsilon/\varepsilon_{\rm comp}$ are given in table 1 and displayed in fig. 4b. Within experimental uncertainties, the results are identical to those obtained with the atomic deuteron beam and confirm that the effects of Coulomb explosion are negligible for the observed structures.

Finally, triatomic deuteron beams (D_3^+) at energies 30 to 90 keV were used (40 μA maximum current at 30 keV) leading to equivalent deuteron beams of $E_{\rm d}$ = 10 to 30 keV with a nearly threefold increase in current. The higher currents permitted the measurement of the stopping power at the lowest energy ($E_{\rm d}$ = 10 keV) with sufficient statistical accuracy. The energy spread due to Coulomb explosion of this triatomic beam is estimated to be at most $\Delta E_{\rm d}$ = 0.72 keV at $E_{\rm d}$ = 20 keV. The results are presented in table 1 and fig. 4c. Within experimental uncertainties, the results are identical to those obtained with the atomic and diatomic deuteron beams and confirm again that the effects of Coulomb explosion are negligible for the observed structures.

When employing currents significantly lower than the maximum values quoted for the three ion species, the resulting stopping power values were identical within experimental uncertainties indicating that space charge effects are negligible.

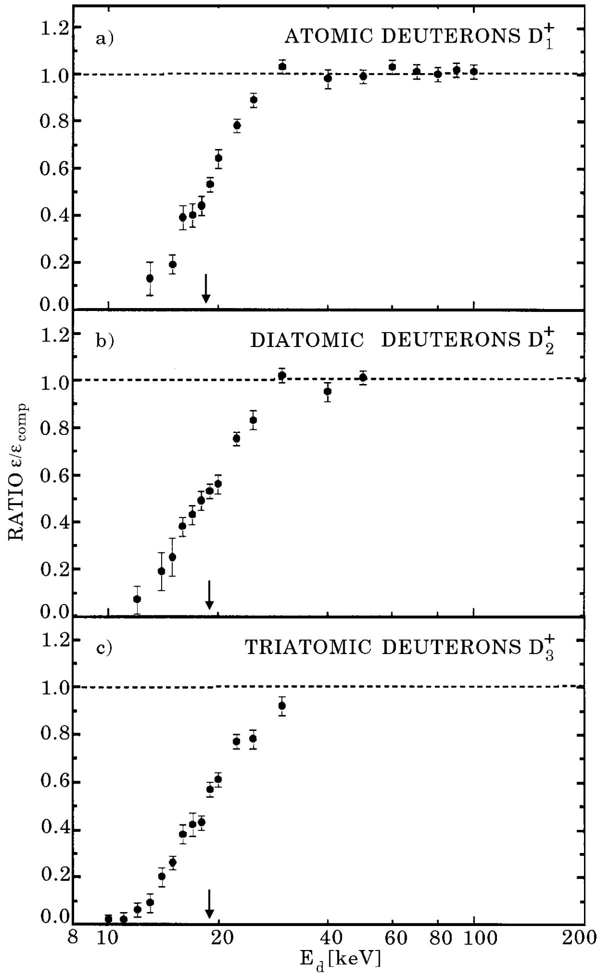

Fig. 4. Stopping power ε of atomic (D_1^+), diatomic (D_2^+), and triatomic (D_3^+) deuterons in ^{3}He gas as a function of atomic deuteron energy and equivalent atomic deuteron energy is compared with the corresponding value $\varepsilon_{\mathrm{comp}}$ from the compilation [3], where for a better comparison only the ratio $\varepsilon/\varepsilon_{\mathrm{comp}}$ is plotted. The arrow indicates the calculated threshold energy $E_{\mathrm{d,min}} = 18.2$ keV.

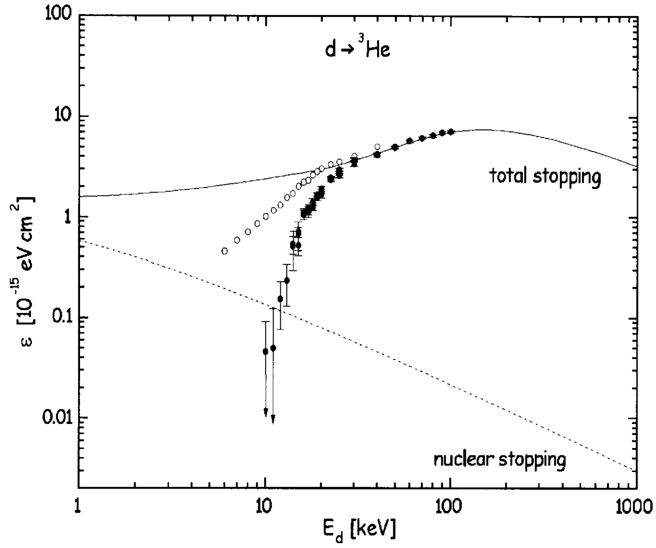

Fig. 5. Stopping power ε of deuterons in ^{3}He gas as a function of the deuteron energy. The total stopping power curve is obtained from the compilation [3] based on data above 80 keV. The nuclear stopping power curve is the prediction from [3]. The filled-circle data points from the present work show a threshold effect near $E_{\mathrm{d}} = 18$ keV. Also shown are the previous results using time-of-flight spectroscopy [5] (open-circle data points).

The combined results for all three deuteron beams are summarized in fig. 5. The observed slope in the stopping power values near $E_{\mathrm{d}} = 18$ keV is much larger than the energy spread of the incident beam, the spread induced by the Coulomb explosion, and the thermal Doppler broadening (*e.g.* 80 eV at $E_{\mathrm{d}} = 20$ keV and $T = 293$ K).

Preliminary data [6] have been obtained only with an atomic deuteron beam, where the results are identical to the present data except for the two lowest energy points ($E_{\mathrm{d}} = 15$ and 18 keV) due to poor statistics and instability of the detectors in the preliminary studies.

4 Discussion

The present stopping power values are significantly different from those reported [5], both in the absolute scale and the energy dependence (fig. 5); this discrepancy is not understood. The present data show a relatively steep drop deviating from the compiled values by 50% near $E_{\mathrm{d}} = 18$ keV (fig. 4), which we define as a threshold energy. The values at lower energy reach the domain of nuclear stopping power according to [3]. In a simple model, the threshold in the electronic stopping power arises from the minimum energy transfer $E_{\mathrm{e,min}}$ in the $1s \rightarrow 2s$ electron excitation of the He target atoms, $E_{\mathrm{e,min}} = 19.8$ eV, which translates into a minimum deuteron energy $E_{\mathrm{d,min}} = (m_{\mathrm{d}}/4m_{\mathrm{e}})(1 + m_{\mathrm{e}}/m_{\mathrm{d}})^2 \mathrm{E}_{\mathrm{e,min}} = 18.2$ keV (m_{d} = deuteron mass, m_{e} = electron mass). Below this energy, the electron cloud of the He atom cannot be excited via an ion-electron interaction and, thus, the electronic stopping power vanishes: the He atoms become transparent for the deuterons. Between $E_{\mathrm{e,min}}$ and the ionisation energy $E_{\mathrm{i}} = 24.6$ eV (corresponding to $E_{\mathrm{d}} = 22.6$ keV), many electronic states in the He atom can be excited leading possibly to the rise in the stopping power near these deuteron energies (fig. 5). Below the threshold energy, one might have expected a sharp drop of the stopping power down to the nuclear stopping power regime. The data show, however, a smoother drop, which is presently not understood. It could possibly arise from a two-step process: inelastic scattering within the nuclear ("atomic") stopping power mechanism could raise electrons to excited atomic states, which in turn could then be further excited by the electron-deuteron interaction. Alternatively, the slope may arise from the coupling of the electron to the He atom, where the electron possesses a momentum distribution leading to three-body effects [13], the so-called Compton profile. The observed values at the lowest energies indicate (fig. 5) that the theoretical values of the nuclear stopping power are significantly overestimated according to [3]. Theoretical calculations are highly desirable to clarify the origin of the threshold effect and the lower values of the nuclear stopping power.

To our knowledge, a relatively sharp threshold effect in the stopping power behavior of ions in matter —as seen in figs. 4 and 5— has not been predicted ([3] and references therein). A threshold effect has been discussed for the stopping power of protons in Ne gas [14], however, these theoretical studies led to an electronic stopping power which depended on the square of the projectile velocity, *i.e.* no sharp threshold was predicted. Similar arguments apply to [15–17], where non-resonant electron capture from He(1s) into the H(1s) shell was suggested as the major energy loss mechanism for protons (deuterons) in He gas at low energies. The observed threshold behavior (figs. 4 and 5) appears in our model to be a quantum effect and may be compared in a way with superconductivity, where matter is transparent to electrons; it is also comparable to X-ray absorption near the K-edge.

On the basis of our model, the observed threshold behavior may occur in many ion-target combinations. For the case of ^{3}He ions in D_2 molecular gas, the D_2 molecule can be dissociated involving an energy of about 0.6 eV with a corresponding threshold energy near $E_{3\mathrm{He}} =$ 0.8 keV; above this energy one may expect no significant deviation from the compilation, as observed [4]. For the case of ^{3}He ions in ^{3}He gas and using the reaction yield of ^{3}He(^{3}He,2p)^{4}He, one expects the threshold energy to be near $E_{3\mathrm{He}} = 27$ keV, and in the case of ^{7}Li ions in ^{3}He gas together with the reaction yield of ^{3}He(^{7}Li,d)^{8}Be one expects a threshold at $E_{7\mathrm{Li}} = 63$ keV. However, the cross-section in both cases at energies far below the height of the Coulomb barrier was too low for an experimental investigation (less than 1 event per month). Although the yield of nuclear reactions at subcoulomb energies is useful in obtaining stopping power data at energies below the Bragg peak, the method cannot be used to study threshold effects in other ion-target systems.

In metallic targets, there should be —on the basis of our model— no threshold effect at all, since the electrons can be excited continuously within overlapping or partially filled energy bands. However, in insulators or semiconductors with separated band gaps, the threshold effect should exist. For the stopping of muons in kapton, an insulator with an electron binding energy of about 2 eV (equivalent to a band gap), a threshold effect has been reported indeed at an energy of about 100 eV [18], near the expected value ($E_\mu \approx 100$ eV).

This work was supported in part by INFN, BMBF (06BO812), DFG (436UNG113-146) and OTKA (T025465).

References

1. W.A. Fowler, Rev. Mod. Phys. **56**, 149 (1984).
2. C. Rolfs, W.S. Rodney, *Cauldrons in the Cosmos* (University of Chicago Press, Chicago, 1988).
3. H. Andersen, J.F. Ziegler, *The Stopping and Ranges of Ions in Matter* (Pergamon, New York, 1977) and SRIM-2000.
4. H. Costantini et al., Phys. Lett. B **482**, 43 (2000).
5. R. Golser, D. Semrad, Phys. Rev. Lett. **66**, 1831 (1991); Nucl. Instr. Meth. B **69**, 18 (1992).
6. A. Formicola et al., Eur. Phys. J. A **8**, 443 (2000).
7. M. Aliotta et al, Nucl. Phys. A (in press).
8. B. Meierjohann, W. Seibt, Z. Phys. **225**, 9 (1969).
9. B. Meierjohann, M. Vogler, J. Phys. B **9**, 1801 (1976).
10. M. Vogler, W. Seibt, Z. Phys. **210**, 337 (1968).
11. M. Vogler, B. Meierjohann, Z. Phys. A **283**, 11 (1977).
12. M. Vogler, B. Meierjohann, J. Chem. Phys. **69**, 2450 (1978).
13. M.E. Rudd et al., Atomic Data and Nuclear Data Tables **18**, 413 (1976).
14. D. Semrad, Phys. Rev. A **33**, 1646 (1986).
15. P.L. Grande, G. Schiwietz, Phys. Rev. A **47**, 1119 (1993).
16. M. Kimura, Phys. Rev. A **47**, 2393 (1993).
17. G.H. Olivera et al., Phys. Rev. A **49**, 603 (1994).
18. H. Daniel et al., Phys. Lett. A **191**, 155 (1994).